

Synthesis of High Yield, Crystalline and Thermally Stable Rare Earth (Sm, Eu, Gd) Oxide Square Nanoplates for Near-Infrared Light Activatable Photocatalysis

Sanjeevan Rajagopal[#], Suresh Thangudu[#] and Kuo Chu Hwang^{*}

Department of Chemistry, National Tsing Hua University, Hsinchu 30013, Taiwan, R.O.C.

Corresponding author email: kchwang@mx.nthu.edu.tw

[#] Authors contributed equally.

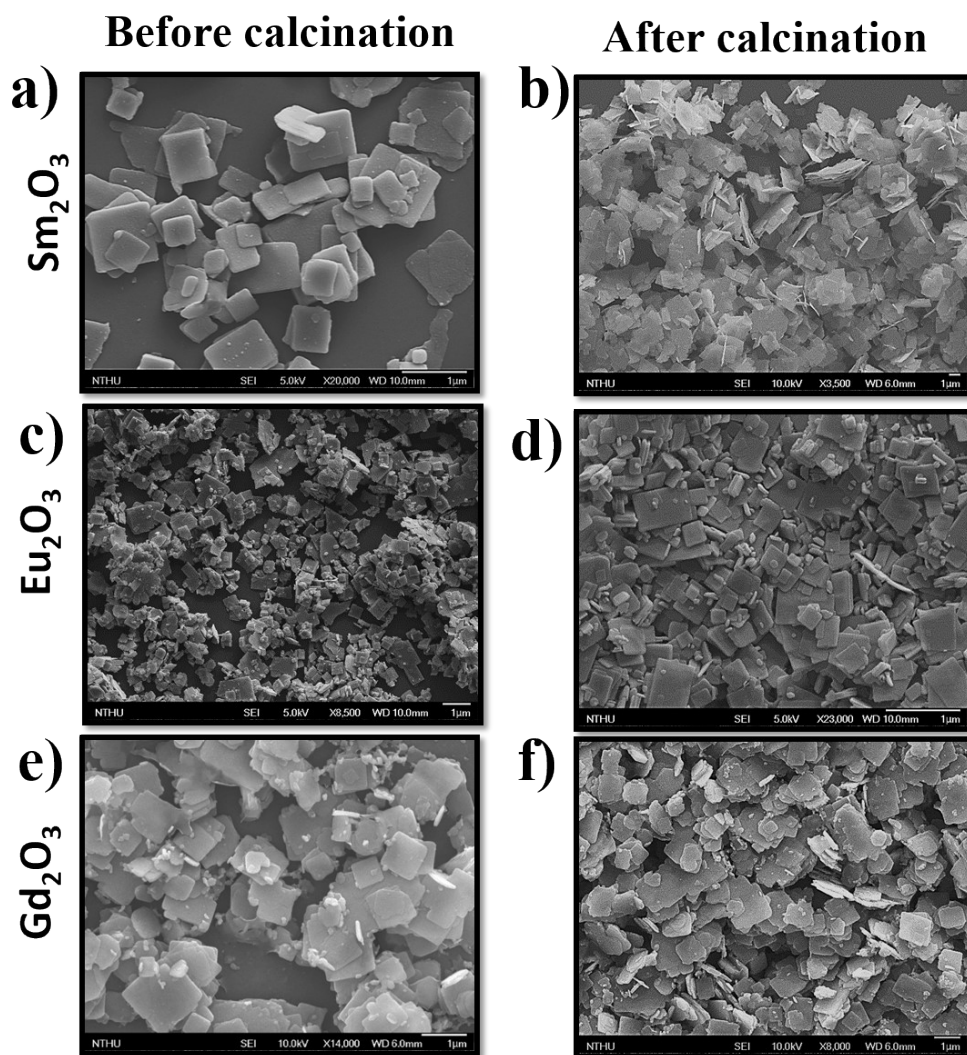


Figure S1 . SEM analysis of REO SNPs (before and after calcination).

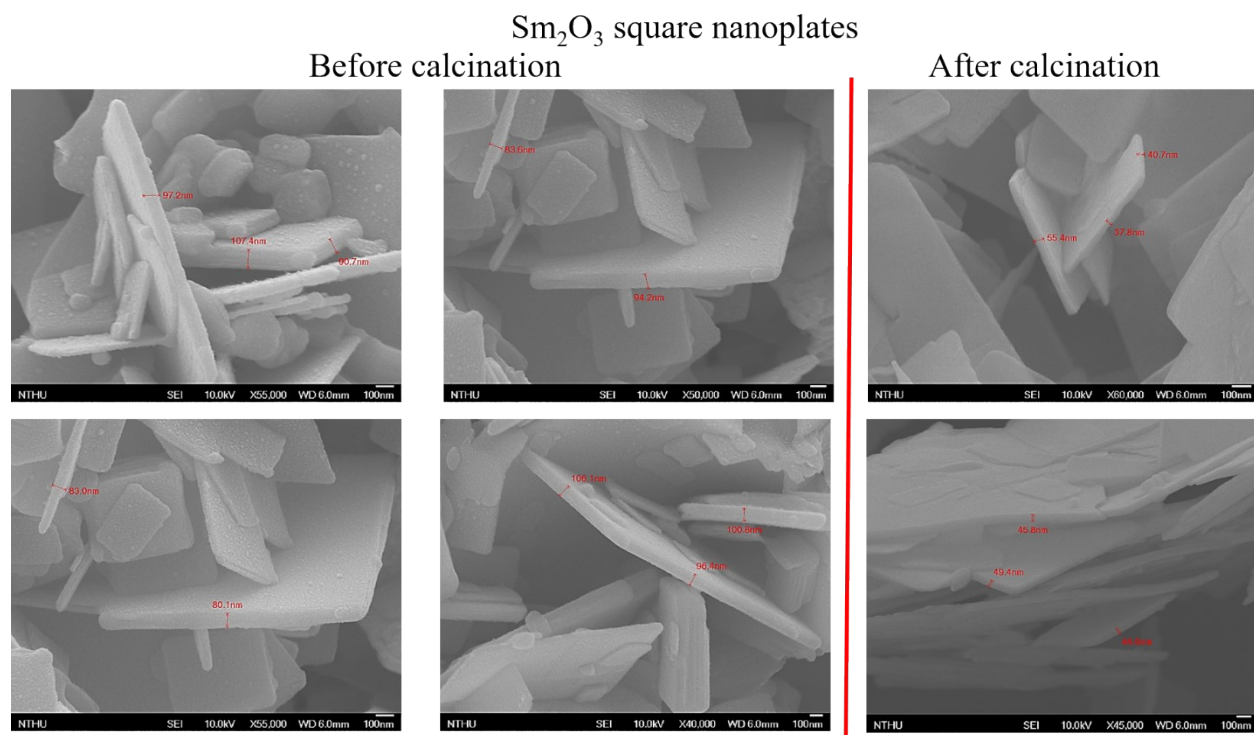


Figure S2. Average thickness of Sm_2O_3 SNPs, before and after calcination treatment at same scale bar.

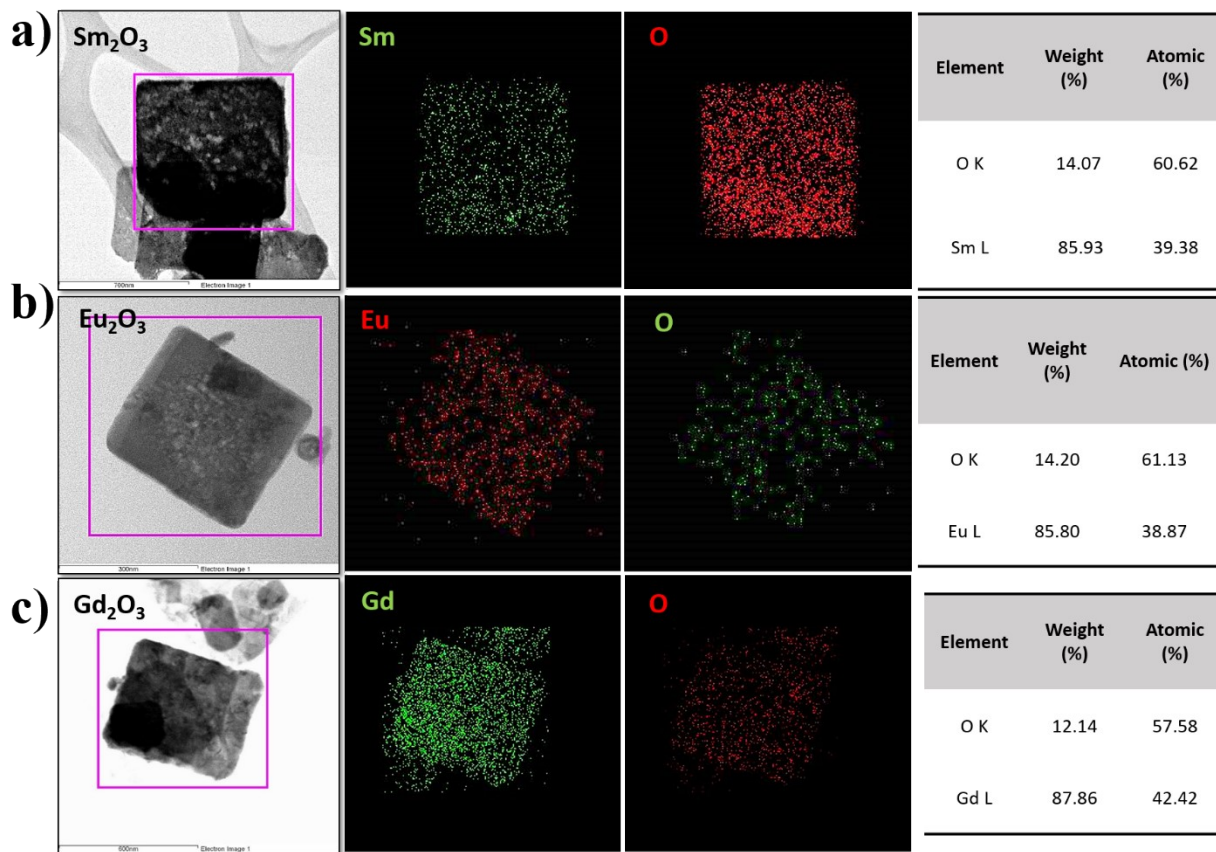


Figure S3. TEM-EDX analysis of calcinated REO SNPs.

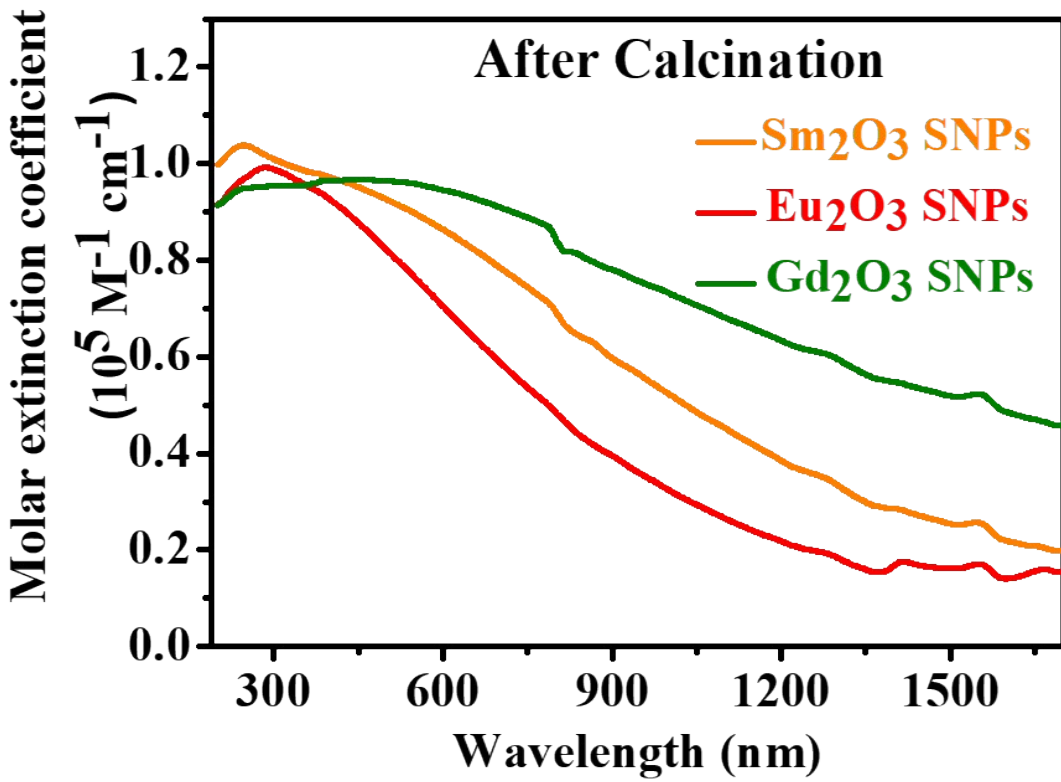


Figure S4. Molar extinction coefficient absorption spectra of REO SNP's.

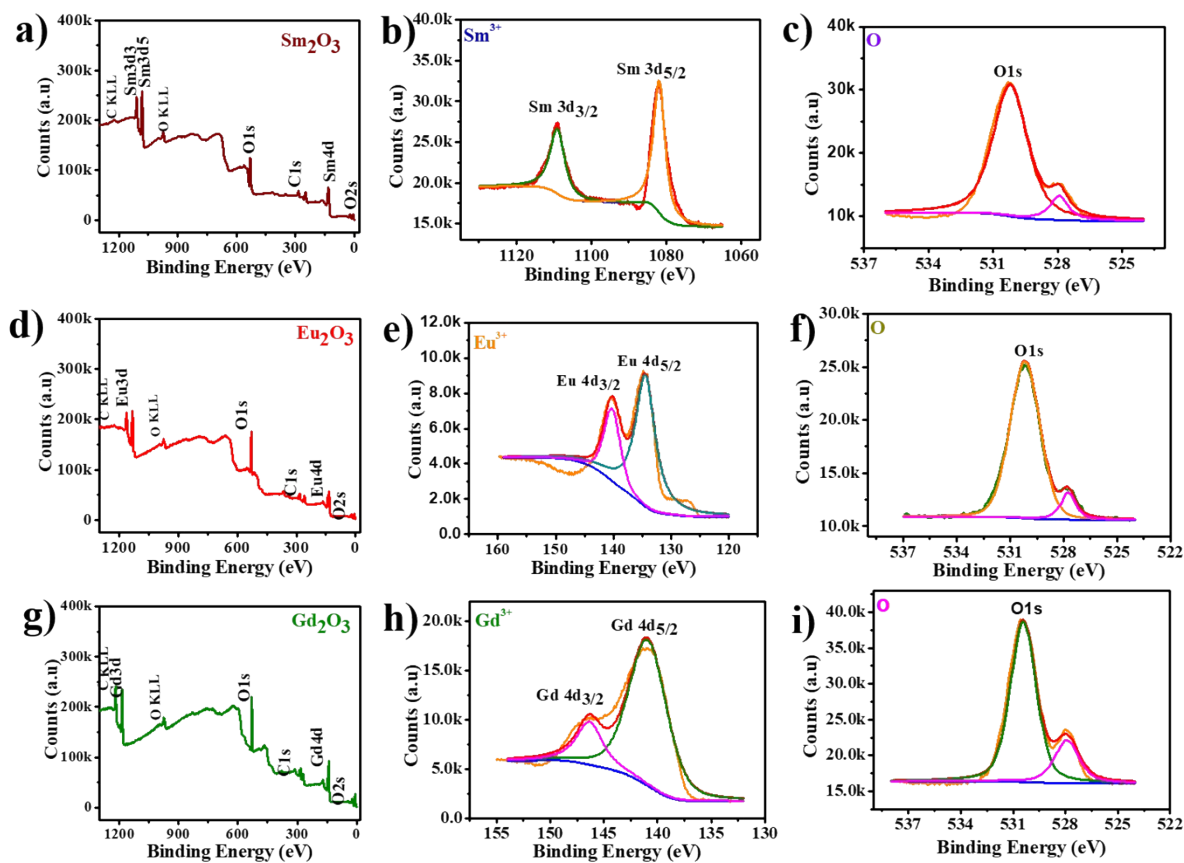


Figure S5. XPS analysis of calcinated REO SNPs. (a) survey scan Sm_2O_3 (b) high-resolution of Sm 3d, (d) Survey scan Eu_2O_3 (e) high-resolution of Eu 4d, (g) survey scan Gd_2O_3 (h) high-resolution of Gd 4d, (c, f, i) high-resolution REO square nanoplates of O 1s.

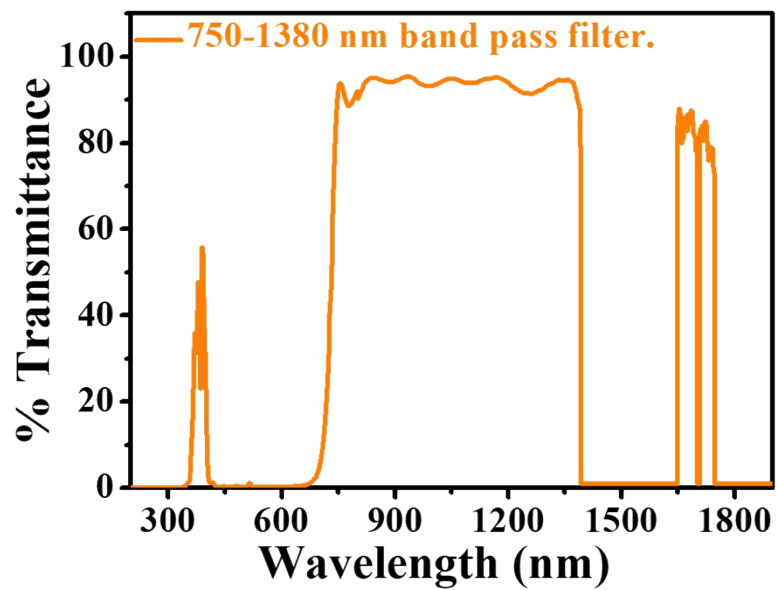


Figure S6. The transmittance spectrum of the output from a halogen lamp after a NIR long-pass filter (750-1380 nm filter).

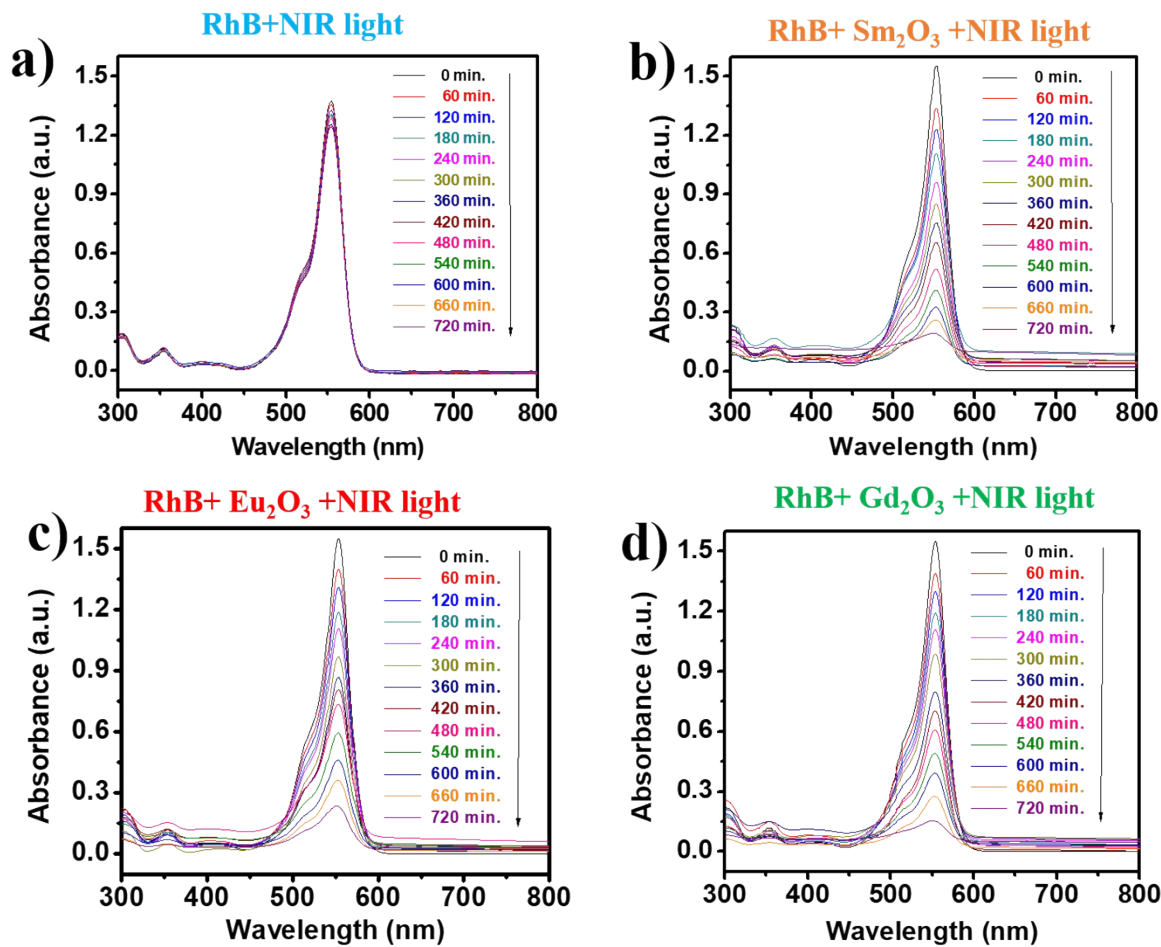


Figure S7. UV-Vis-NIR absorbance spectrum different time point absence and presence of a catalyst (a) without catalyst RhB with NIR light (b) with catalyst (without calcination) Sm₂O₃ RhB, NIR light (c) with catalyst (without calcination) Eu₂O₃ RhB, NIR light (d) with catalyst (without calcination) Gd₂O₃ RhB, NIR light.

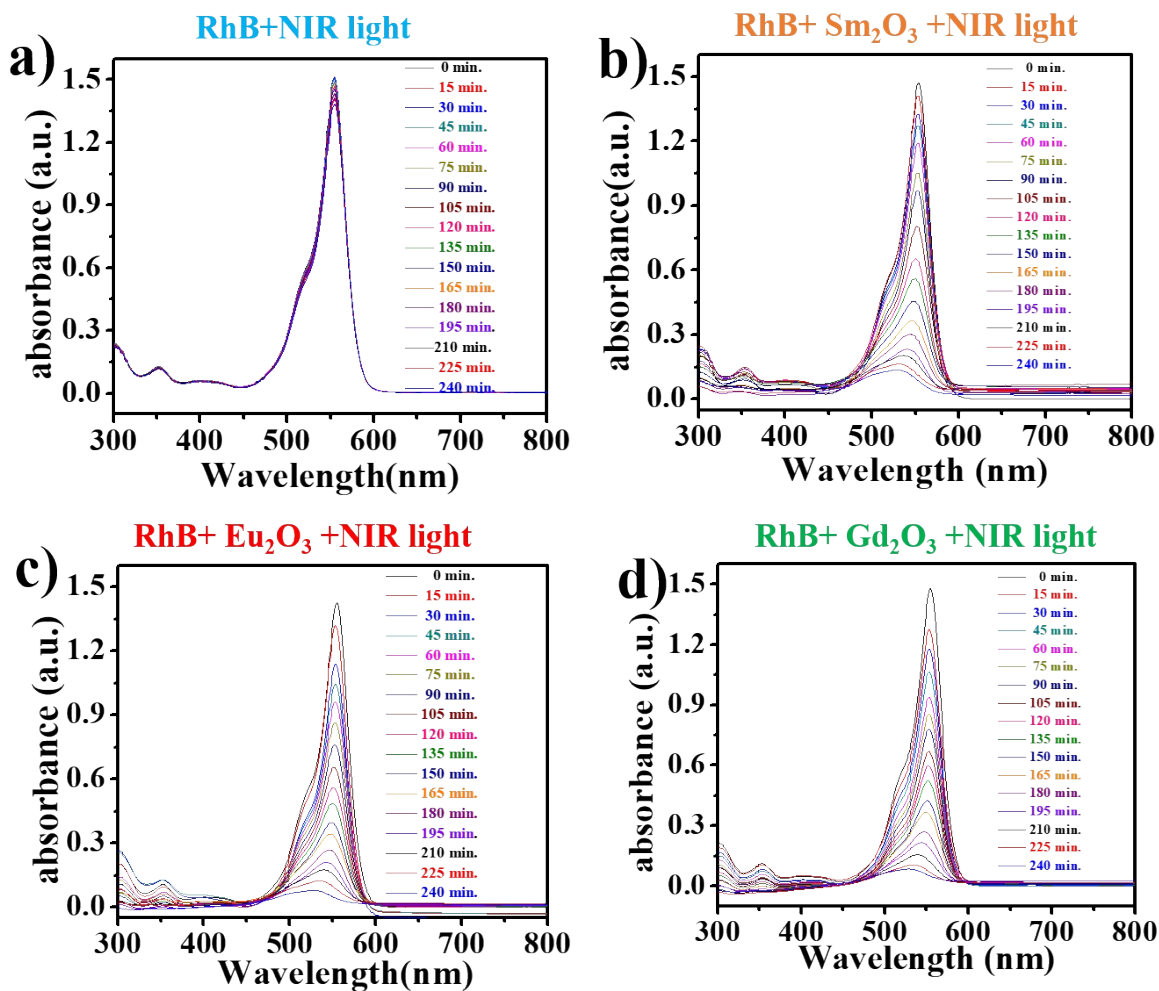


Figure S8. UV-Vis-NIR absorbance spectrum absence and presence of a catalyst at a different time point (0 -240 min.) (a) Without catalyst RhB with NIR light (b) with calcination catalyst Sm_2O_3 RhB, NIR light (c) with calcination catalyst Eu_2O_3 RhB, NIR light (d) with calcination catalyst Gd_2O_3 RhB, NIR light.

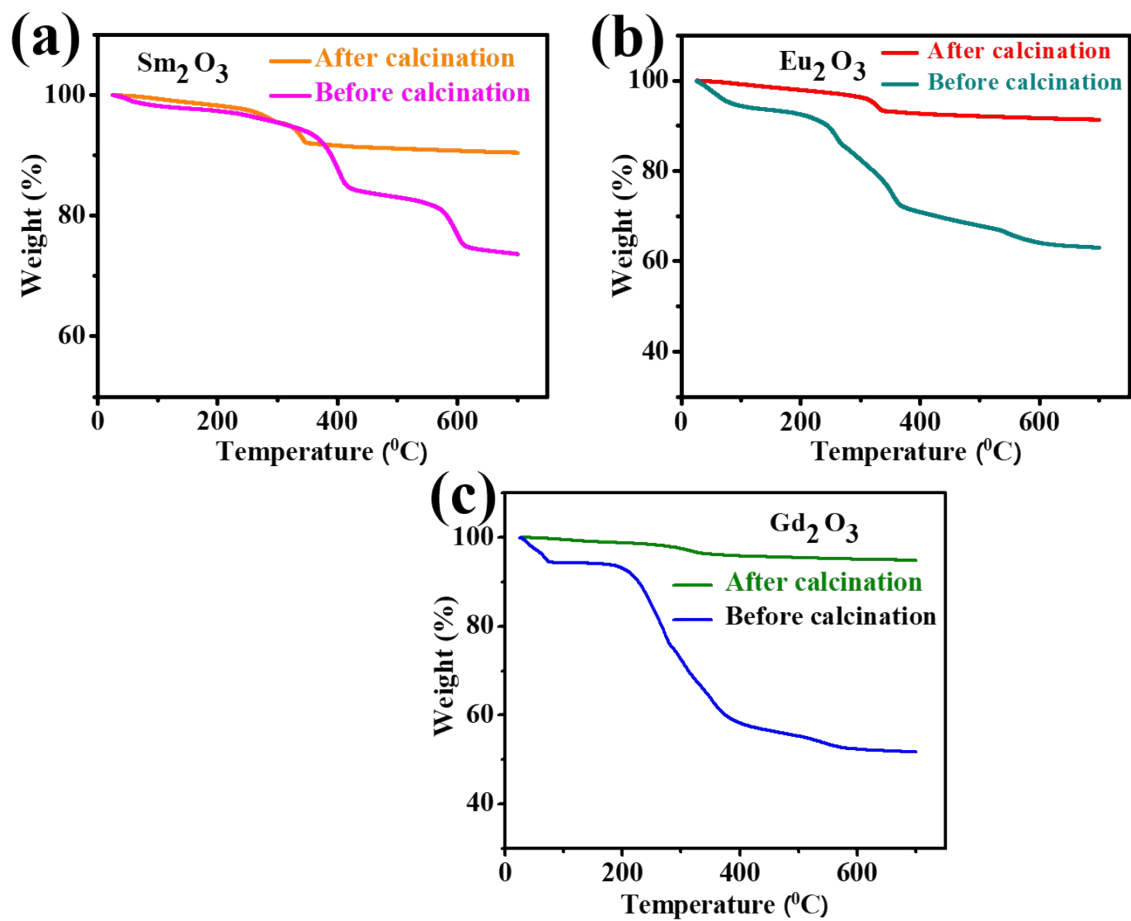


Figure S9. Thermogravimetric analysis of as synthesized SNPs a) Sm₂O₃, b) Eu₂O₃, c) Gd₂O₃. (Condition: room temperature to 750 °C with a heating rate of 10 °C/min).

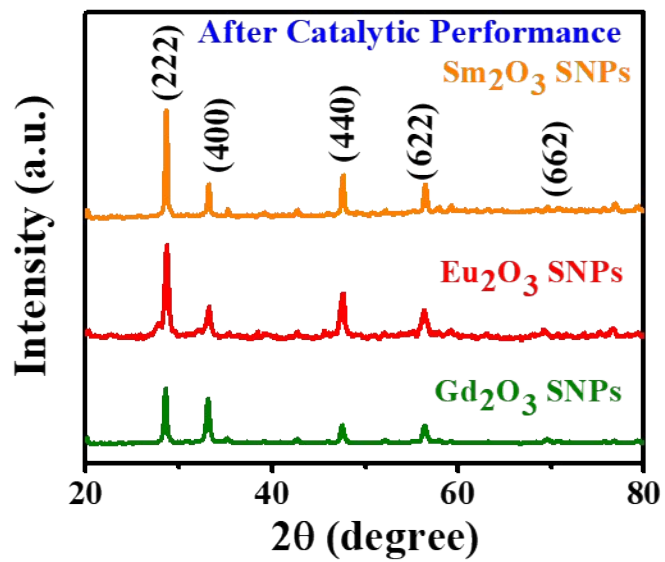


Figure S10. XRD analysis of REO SNPs after photocatalytic reaction.

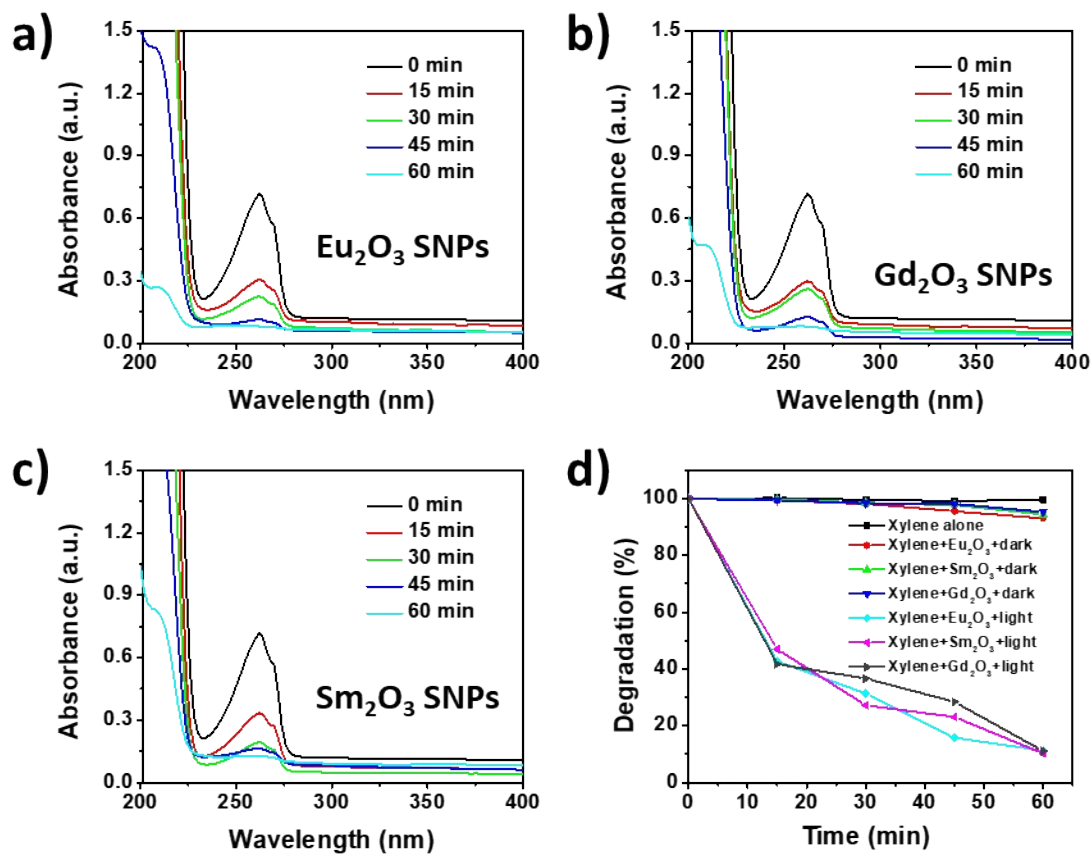


Figure S11. Photocatalytic degradation of o-xylene on REO SNPs (experimental condition: 1 mg/mL catalyst, 50 W halogen lamp fitted with a NIR filter)

Table S1 Summary of recent developments on NIR light photocatalysis.

Photocatalysis	Organic pollutant dye	Irra. time(hrs)	Laser	Efficiency	Reference
BiWO ₆ nanosheets	Methyl orange	2	980 nm	75 %	S1
Cu(OH)PO ₄ microcrystals	2,4-dichlorophenol	6	λ>800 nm	90 %	S2
NaYF ₄ :Yb, Tm@TiO ₂ core-shell NPs	Methyl blue	14	980 nm	65 %	S3
BiVO ₄ /CaF ₂ :Er ³⁺ , Tm ³⁺ , Yb ³⁺ NPs.	Methyl orange	6	980 nm	40 %	S4
Ag ₂ S/Ag ₃ PO ₄ core/shell	Methyl orange	2	760 nm	90 %	S5
YF ₃ :Yb,Tm/TiO ₂	Methyl blue	30	980 nm	70%	S6
CaF ₂ :Yb@BiVO ₄	Methyl orange	7	980 nm	70%	S7
MoO ₃ nanobelts	Rhodamine B	2	800–1600 nm	70 %	S8
β-NaYF ₄ :Yb/Er-N-TiO ₂	Rhodamine B	36	980 nm	80%	S9
Rare Earth Oxides Sm ₂ O ₃ , Eu ₂ O ₃ , and Gd ₂ O ₃ square nanoplates	Rhodamine B	6	750–1350 nm	92 % 95 % 96 %	Present work

Supplementary References

S1. J. Tian, Y. Sang, G. Yu, H. Jiang, X. Mu and H. Liu, *Adv. Mater.*, 2013, **25**, 5075–5080.

S2. G. Wang, B. Huang, X. Ma, Z. Wang, X. Qin, X. Zhang, Y. Dai and M. H. Whangbo, *Angew. Chem., Int. Ed.*, 2013, **52**, 4810–4813

- S3.** Y. Tang, W. Di, X. Zhai, R. Yang and W. Qin, *ACS Catal.*, 2013, **3**, 405– 412.
- S4.** S. Huang, N. Zhu, Z. Lou, L. Gu, C. Miao, H. Yuan and A. Shan, *Nanoscale*, 2014, **6**, 1362-1368.
- S5.** J. Tian, T. Yan, Z. Qiao, L. Wang, W. Li, J. You and B. Huang, *Appl. Catal., B*, 2017, **209**, 566–578.
- S6.** W. Qin, D. Zhang, D. Zhao, L. Wang and K. Zheng, *Chem. Commun.*, 2010, **46**, 2304–2306.
- S7.** X. Liu, W. Di and W. Qin, *Appl. Catal., B*, 2017, **205**, 158–164.
- S8.** C. Hu, M. Xu, J. Zhang, Y. Zhou, B. Hu, and G. Yu, *International Journal of Chemical Kinetics*, 2019, **51**, 3-13.
- S9.** Y. Ma, W. Yue, Z. Xu, Z. Ye, and J. Zhang, *Catalysis Today*, 2023, **410**, 13-18.